Published as: *Science*. 2025 February 07; 387(6734): 666–673.

Moisture-responsive root-branching pathways identified in diverse maize breeding germplasm

Johannes D. Scharwies[1,*], **Taylor Clarke**[1], **Zihao Zheng**[3,†], **Andrea Dinneny**[1], **Siri Birkeland**[4,‡], **Margaretha A. Veltman**[5,§,¶], **Craig J. Sturrock**[6], **Jason Banda**[6], **Héctor H. Torres-Martínez**[1], **Willian G. Viana**[1], **Ria Khare**[7], **Joseph Kieber**[7], **Bipin K. Pandey**[6], **Malcolm Bennett**[6], **Patrick S. Schnable**[3], **José R. Dinneny**[1,2,*]

[1]Department of Biology, Stanford University; Stanford, CA 94305, USA.

[2]Howard Hughes Medical Institute, Stanford University; Stanford, CA 94305, USA.

[3]Department of Agronomy, Iowa State University; Ames, IA 50011-1085, USA.

[4]Faculty of Chemistry, Biotechnology and Food Science, Norwegian University of Life Sciences; Ås, 1432, Norway.

[5]Natural History Museum, University of Oslo; Oslo, 0318, Norway.

[6]Plant and Crop Sciences, School of Biosciences, University of Nottingham; Sutton Bonington, LE12 5RD, UK.

[7]Department of Biology, University of North Carolina; Chapel Hill, NC 27599, USA.

Abstract

Plants grow complex root systems to extract unevenly distributed resources from soils. Spatial differences in soil moisture are perceived by root tips leading to the patterning of new root branches towards available water, a process called hydropatterning. Little is known about

[*]Corresponding author. joscha@stanford.edu (J.D.S), dinneny@stanford.edu (J.R.D).
[†]Present address: Vegetable & Flower Seeds Development, Syngenta Crop Protection LLC; NC 27709, USA.
[‡]Present address: Natural History Museum, University of Oslo; Oslo, 0318, Norway.
[§]Present address: Institut de Recherche pour le Développement; 34394 Montpellier, France.
[¶]Additional affiliation: Naturalis Biodiversity Center; 2333 CR Leiden, The Netherlands.

Author contributions:
Conceptualization: JDS, JRD
Data acquisition: JDS, TC, AD, CJS, JB, HHT-M, WGV
Data analysis: JDS, ZZ, SB, MAV
Visualization: JDS, CJS, SB, MAV
Resources: RK, JK, BKP, MB, PSS
Funding acquisition: JRD, JK, BKP, PSS, CJS, JB, MB, MAV, SB
Project administration: JDS
Supervision: JDS, JRD
Writing – original draft: JDS, JRD
Writing – review & editing: all authors

Supplementary Materials
Materials and Methods
Figs. S1 to S9
References (43–72)
Supplementary Data S1 to S16

hydropatterning behavior and its genetic basis in crops plants. Here, we develop an assay to measure hydropatterning in maize and reveal substantial differences between tropical/subtropical and temperate maize breeding germplasm that likely resulted from divergent selection. Genetic dissection of hydropatterning confirmed the regulatory role of auxin and revealed that the gaseous hormone ethylene locally inhibits root branching from air-exposed tissues. Our results demonstrate how distinct signaling pathways translate spatial patterns of water availability to developmental programs that determine root architecture.

Climate change is predicted to increase the duration and severity of droughts (1). This will threaten crop production, which depends heavily on water. Plant water uptake is facilitated by an intricate network of roots. Breeding plants with improved root access to water is a potential method to make crops resilient to climate change (2). Root networks are established by branching of the primary root axis. The development of lateral root branches is highly responsive to the spatio-temporal distribution of resources like water and nutrients in soils (3, 4). Plants sense micron-scale heterogeneity in water availability at their root tips with spatial differences along the root-tip circumference determining the patterning of lateral roots through hydropatterning (5, 6) (Fig. 1A). This response may allow plants to capture water more efficiently while minimizing the metabolic cost of root growth in dry soil (7). Understanding the extent of phenotypic variation for this trait within breeding populations and determining its genetic basis may facilitate crop improvement. Furthermore, understanding the mechanistic basis of hydropatterning illuminates how heterogeneity in moisture is sensed by organisms to enact an adaptive response.

Hydropatterning in domesticated maize

Here we investigated hydropatterning in the cereal crop species *Zea mays* (maize), which constitutes a major source of calories worldwide. To capture the phenotypic diversity of hydropatterning, we developed an assay using germination paper to create a controlled gradient of water availability across the circumference of the growing primary root (Fig. 1B and fig. S1). Simultaneous characterization of a diverse set of 250 maize inbred lines (data S1) from the Goodman-Buckler association panel allowed us to cover the majority of genetic diversity present in current public-sector breeding programs (8).

For all tested maize inbred lines, we observed that primary roots preferentially formed lateral roots on the side touching the water-saturated germination-paper (contact-side), which is consistent with the inductive effect of water availability previously observed in the maize reference inbred B73 and in other species (5) (Fig. 1C, data S2). Nevertheless, a substantial proportion of all surveyed maize inbred lines developed air-side lateral roots as well, resulting in an observed phenotypic range of 0 – 39% air-side lateral roots across all 250 inbred lines (Fig. 1D). This suggests that a larger portion of maize inbred lines exhibit weakened hydropatterning (more air-side lateral roots) than previously indicated (9). Additionally, we observed in a set of 20 maize inbred lines with diverse hydropatterning responses in primary roots, that hydropatterning in crown roots, which make up the bulk of mature maize root systems, is significantly correlated (fig. S2, A to C and data S3). Our results highlight the substantial variation of hydropatterning across maize root types,

allowing this trait to be used for understanding how quantitative genetic variation contributes to overall root architecture.

In the B73 maize inbred line, lateral root founder cells are initiated around 12 mm from the root tip (10). Prior research using B73 found that moisture availability cues, which determine the patterning of lateral roots, are perceived closer to the root tip, specifically within the first 5–6 mm (9). This suggests that moisture cues act on lateral root development at the founder cell patterning stage rather than at later developmental stages. Comparing lateral root patterning in several strong (< 5% air-side lateral roots) and weak (> 20% air-side lateral roots) hydropatterning inbred lines, we found that pre-emerged lateral root primordia and post-emergence lateral roots exhibited the same bias in distribution between contact- and air-sides corresponding to the hydropatterning strength of each inbred line (fig. S2, D and E). Our observations provide further evidence that hydropatterning primarily acts at the lateral root founder cell patterning stage.

We next examined how the observed variation in hydropatterning correlates with root architecture in soil conditions. In nature, large air-spaces in the soil matrix, called macropores, are commonly created by prior root growth or burrowing invertebrate activity, such as by earthworms. We tested how lateral roots were patterned when primary roots were grown through artificial macropores. Strong hydropatterning inbred lines initiated their lateral roots preferentially towards the side of the root in contact with soil, as observed by microscale X-ray Computed Tomography (Fig. 1E). In contrast, weak hydropatterning inbred lines displayed a reduced bias with more lateral roots growing into the air-filled macropore. Quantification across multiple strong and weak hydropatterning inbred lines found that they made similar percentages of air-side lateral roots in the soil macropore and our hydropatterning assay (fig. S2, F to H). The results demonstrate that our hydropatterning assay generates reproducible phenotypes that translate to soil conditions.

To explore how variation in hydropatterning relates to other phenotypic traits of field-grown maize plants, we performed a correlation analysis with 64 compiled trait sets measured from field-grown plants (11). We found that both air-side lateral root density and percent air-side lateral roots correlate significantly with root crown depth and the number of nodes with brace roots (fig. S3, A to C and data S4). Weaker hydropatterning inbred lines generally exhibited more shallow root systems with fewer brace roots according to data collected by two studies from Iowa (fig. S3, D to F) (12, 13). This suggests that more efficient placement of root branches towards water may improve the ability of root systems to attain greater depths, possibly due to the metabolic savings achieved by limiting branching in dry soil (14). Importantly, no significant correlations were observed with contact-side lateral root density, suggesting that this trait has less relevance to the in-field root architecture traits measured.

Variation and selection of hydropatterning across maize breeding subpopulations

We reassessed population structure and assigned subpopulations for all phenotyped inbred lines that had matching whole-genome sequencing data available (n = 231). Inbred lines

with less than 80% subpopulation identity were assigned to a mixed group (8) (Fig. 2A and data S5). While variation in contact-side lateral root density was uniform across all subpopulations, inbred lines with higher air-side lateral root density and percent air-side lateral roots were predominantly associated with the non-stiff stalk/mixed groups (Fig. 2, B to D). This led to significantly weaker hydropatterning for the large temperate non-stiff stalk group compared to the large tropical/subtropical group or the smaller temperate stiff stalk group (Fig. 2E and fig. S4A).

To test whether this divergence in hydropatterning was best explained by neutral evolution or selection, we compared quantitative genetic differentiation with regards to contact- or air-side lateral root density (Q_{ST}) to the population genetic differentiation due to genetic structure (F_{ST}). We found that Q_{ST} and F_{ST} distributions overlapped for contact-side lateral root density, which suggests that genetic differentiation for this trait occurred through neutral evolution. Conversely, Q_{ST} was significantly in excess of F_{ST} for air-side lateral root density, as well as percent air-side lateral roots, indicating divergence through differential selection for these hydropatterning traits (Fig. 2F, fig. S4B, and data S6). Pairwise comparisons between subpopulations show the largest Q_{ST} - F_{ST} differences between the non-stiff stalk and tropical/subtropical groups, suggesting that divergence in selective pressures for hydropatterning occurred predominantly after the split between tropical/subtropical and temperate germplasm (Fig. 2G, fig. S4C, and data S6). Stronger hydropatterning in the tropical/subtropical subpopulation may have resulted from selection for drought tolerance, among other abiotic stress factors, during breeding (15, 16). In contrast, weakened hydropatterning in the temperate non-stiff stalk subpopulation could be the result of relaxation in selection pressures on efficient water uptake in temperate environments. However, linkage between hydropatterning and other traits could have contributed to differences in hydropatterning between subpopulations. Pronounced $Q_{ST} > F_{ST}$ differences for air-side lateral root density and contrasting observations for contact-side lateral root density support our hypothesis but inbreeding may inflate Q_{ST} estimates (17).

Genetic architecture of hydropatterning in domesticated maize

Previous work in *Arabidopsis thaliana* (Arabidopsis) has shown that the auxin hormone signaling pathway promotes branching on the contact-side of roots during hydropatterning. Mutants that disrupt auxin biosynthesis and polar transport are known to weaken hydropatterning (5). Similar to Arabidopsis, we found in maize that auxin accumulates preferentially on the contact-side of hydropatterning roots which creates a bias for lateral root induction (fig. S5). Furthermore, it has been shown that the auxin-response transcription factor AUXIN RESPONSE FACTOR 7 (ARF7) is sumoylated in cells on the air-side of roots, promoting binding to the repressor protein INDOLE-3-ACETIC ACID INDUCIBLE 3 (IAA3) which blocks initiation of lateral root founder cells (18). To identify novel loci and associated genes for hydropatterning with relevance to maize, we conducted Genome and Transcriptome Wide Association Studies (GWAS/TWAS), which associate single nucleotide polymorphisms, or variation in gene expression amongst the study population, to variation in a trait of interest.

TWAS (13) identified nine genes whose expression in germinating seedling roots (19) is significantly associated with differences in air-side lateral root density (Fig. 3A and data S7). Among these TWAS-genes, we found *Zm00001eb211770*, a maize ortholog of *AUXIN RESISTANT 1* (*ZmAXR1*). In Arabidopsis, AXR1 together with E1 C-terminal related 1 (ECR1) act as ubiquitin-activating enzymes that facilitate the RUB modification of CULLIN 1 (CUL1) which is part of the $SCF^{TIR/AFB}$ complex at the center of auxin perception. RUB modification is necessary to allow auxin signal transduction for lateral root induction (20). TWAS in maize found that higher gene expression of *ZmAXR1* is associated with increased air-side lateral root densities (fig. S6A, data S7) which may be due to an increased sensitivity for auxin perception leading to more frequent induction of lateral roots on the air-side. To analyze the origin of the variation in *ZmAXR1* gene expression, we mapped the associated expression Quantitative Trait Loci (eQTL). This analysis revealed several significant expression-associated Single Nucleotide Polymorphisms (e-SNP) (fig. S6B, data S8 and 9). The most significant e-SNP, Chr5_2705946, co-localized with *ZmAXR1* itself, indicating that cis-acting regulatory variation may explain the variation in *ZmAXR1* gene expression associated with air-side lateral root density. Input data for the TWAS suggested expression of *ZmAXR1* in root tips of most inbred lines (fig. S6A). This was confirmed through in situ detection of *ZmAXR1* transcripts in root tips of maize inbred line B73 by Hybridization Chain Reaction (fig. S7, B and C). These results indicate that auxin regulation and related processes play a role in hydropatterning for maize roots as previously demonstrated in Arabidopsis (5, 18).

In parallel, GWAS (21, 22) identified 30 unique Trait-Associated SNPs (TASs) for air-side lateral root density (Fig. 3B, fig. S6 C and D, and data S10), suggesting that variation in hydropatterning is controlled by numerous loci in maize. In almost all cases, higher air-side lateral root density was associated with the less frequent allele (minor allele) of the TAS within our population, except for TAS Chr8_143668219, as shown by the effect estimate (data S10). This supports our hypothesis that weakening of hydropatterning may have been caused by relaxation of selection, since selection typically constrains the occurrence of genetic variants (23). We identified a total of 40 genes within 20-kb windows centered on the TASs. In cases where no gene was located within these windows, the next closest gene was included (data S11). These genes were considered candidates for genes that may control air-side lateral root density in maize.

Validation of maize candidate genes using Arabidopsis orthologs

We identified maize candidate gene orthologs in Arabidopsis, and screened available mutant lines for hydropatterning defects (fig. S8A and data S12 and 13). Screening revealed seven genes for which at least one mutant allele showed a significant change in air-side lateral root density and percent air-side lateral roots (Fig. 3C and fig. S8B). For three of these genes, two independent mutant alleles both showed significant, matching changes in air-side lateral root density, confirming their association with hydropatterning (Fig. 3, D and E)

Auxin signaling pathway mutants *axr1-3* and *axr1-12* of *AtAXR1* showed significant increases in air-side lateral root density and percent air-side lateral roots compared to the wild-type, while contact-side lateral root density dropped significantly (Fig. 3D and E). This

defect is similar to the phenotype of other auxin-pathway mutants in Arabidopsis (5, 18) and confirms that the auxin hormone pathway plays an important role in promoting the bias in lateral root development towards the moisture-contacting side of the root both in Arabidopsis and maize.

Similarly, we observed significant increases in air-side lateral root density and percent air-side lateral roots in Arabidopsis mutants of HMG-CoA REDUCTASE DEGRADATION 3A (*AtHRD3A*), *hrd3a-1* and *hrd3a-2* (Fig. 3D and E). *AtHRD3A*, an ortholog of GWAS candidate *Zm00001eb398230* (*ZmHRD3A*), recruits misfolded proteins for endoplasmic reticulum-associated protein degradation to the HRD1/HRD3 complex (24). Targets include misfolded receptor-like kinases and glycosylated proteins (25), suggesting that hydropatterning may rely upon proteins acting at the plasma membrane that are also targets of endoplasmic reticulum-associated protein degradation. In contrast to mutants of *AtAXR1*, *hrd3a-1* and *hrd3a-2* showed no, or a relatively small, changes in contact-side lateral root densities, respectively. This suggests that HRD3A may primarily function in the suppression of air-side lateral root development. In maize, *ZmHRD3A* was discovered as one of three candidate genes associated with TAS Chr9_147576641 (data S11). Mutants of *At5g16720*, an ortholog of *Zm00001eb398220* associated with the same TAS, did not affect hydropatterning (fig. S7B). *ZmHRD3A* is expressed at the root tip in the same region where moisture signals control the patterning of lateral roots (fig. S7, A and D).

In contrast to *axr1* and *hrd3a*, Arabidopsis mutants of *FASCICLIN-LIKE ARABINOGALACTAN-PROTEIN 4* (*AtFLA4*), named *salt overly sensitive5* (*sos5-1* and *sos5-2*), showed significant strengthening of hydropatterning with decreases in air-side lateral root density and percent air-side lateral roots compared to wild-type (Fig. 3D). The mutant *sos5-1* was identified for its defects in growth on saline media (26). While the primary root phenotype under salinity and ionic stress has been studied extensively (27), no reports have described a lateral root phenotype. *AtFLA4* belongs to a group of 21 fasciclin-like arabinogalactan proteins and carries two fasciclin 1 domains that allow it to interact with the extracellular cell wall matrix (28, 29), which may allow it to sense extracellular cues originating from the environment. The decrease in air-side lateral root density in the *sos5* mutants was accompanied by a significant increase in contact-side lateral root density and a significant reduction in primary root length (Fig. 3E and fig. S9A). Taking this reduction of primary root length into account, *sos5-1* and *sos5-2* both showed a significant decrease in the total number of emerged air-side lateral roots per seedling but only a small or no increase in total contact-side lateral roots per seedling (fig. S9B). Thus, these data indicate that *sos5* primarily suppresses air-side lateral roots, while changes in contact-side lateral root density may result from pleiotropic effects on root length. *AtFLA4* is an ortholog of GWAS candidate *Zm00001eb367960* (*ZmFLA4*), which was discovered as one of four candidate genes associated with TAS Chr8_175425640 (data S11). Similar to *AtFLA4*, *ZmFLA4* contains two fasciclin 1 domains (30). Orthologous Arabidopsis mutants of two other candidate genes associated with the same TAS, *Zm00001eb367970* and *Zm00001eb367990*, showed no defect in hydropatterning (fig. S8B). This provides evidence that variation associated with *ZmFLA4* may be the primary determinant of the observed variation in hydropatterning at TAS Chr8_175425640. In maize, *ZmFLA4* is expressed at the root tip (fig. S7, A and E).

Ethylene as an air-side signal mediating hydropatterning

Ethylene is a gaseous plant hormone that regulates development in response to several abiotic stresses (31). Accumulation of root-produced ethylene in compacted soils serves as a signal leading to root growth inhibition (32). In Arabidopsis, *AtFLA4* may act in a genetic pathway regulating the synthesis of ethylene precursor 1-aminocyclopropane-1-carboxylate (ACC) from S-adenosylmethionine (SAM) (Fig. 4A) (27). In this pathway, AtFLA4 acts upstream of two leucine-rich repeat receptor-like kinases, AtFEI1 and AtFEI2 (33). These kinases interact with 1-AMINOCYCLOPROPANE-1-CARBOXYLATE SYNTHASE (ACS) 5 and 9, which are involved in the synthesis of ACC. Associated with this pathway, ETHYLENE OVERPRODUCER 1 (AtETO1) functions as a negative regulator of type-2 ACS enzymes, including ACS5 and ACS9 (34).

We found that double mutants of *AtFEI1* and *AtFEI2* (*fei1*/*fei2-1*) as well as single mutants of *AtETO1* (*eto1*) and *AtACS5* (*acs5*^{eto2}, which carries a C-terminal mutation in ACS5 that increases protein stability) all showed similar reductions in air-side lateral root density as observed in the *AtFLA4* mutants *sos5-1* and *sos5-2*. Concomitantly, all mutants showed an increase in contact-side lateral root density and a reduction in primary root length (Fig. 4, B to D, and fig. S9, C to E). Screening of the single mutants *fei1* and *fei2-1* revealed no significant effects on air-side lateral root density (fig. S9F), corroborating a suggestion that both genes may act in a redundant fashion (33). While both *eto1* and *acs5*^{eto2} increase ACC synthesis, a reduction of ACC synthesis in the *AtACS* hextuple mutant (*acs2-1, acs4-1, acs5-2, acs6-1, acs7-1, acs9-1*) led to a significant increase in air-side lateral root density (Fig. 4E). We also tested the single mutant *acs5-1*, but observed no difference compared to wild-type (fig. S9G). This result is likely due to the high-level of redundancy between *ACS* genes in Arabidopsis, which has eight functional ACS homologs (35). Our results suggest that genetic modulation of ACC synthesis affects hydropatterning in a way that resembles the phenotypes of *sos5-1* and *sos5-2*.

Next, we asked whether ACC itself or ethylene, which is synthesized from ACC by ACC-oxidases (ACOs), causes the observed repression in air-side lateral root development. We found that treatment with 2-aminoisobutyric acid (AIB), a competitive inhibitor of ACOs, caused an increase in air-side lateral root density and rescued the *sos5-2* mutant phenotype (Fig. 4, F and G). Likewise, treatment of Col-0 wild-type with ACC alone reduced air-side lateral root density, likely due to the increased production of ethylene since this effect was reversed by co-treatment with AIB (Fig. 4H). Both ACC and ACC + AIB treatments showed significant increases in contact-side lateral root density compared to mock treated Col-0 wild-type. These increases could be due to a concomitant reduction in primary root length with both treatments (fig. S9H), and/or potential effects of ACC itself on lateral root induction (36). Taken together, these observations suggest a central role for ethylene in the suppression of air-side lateral root development, which does not require localized ACC synthesis, since exogenous ACC application on the contact-side was able to induce the same effect.

In maize, AIB treatment of a strong hydropatterning inbred line 33–16 increased air-side lateral root density and significantly reduced ethylene production (Fig. 4, I and J). This

indicates that ethylene suppresses air-side lateral root development in maize as well. Measurements of ethylene production from root tips of maize inbred lines that either carry the major or minor allele for TAS Chr8_175425640, localized about 2 kilobases upstream of *ZmFLA4*, showed the minor allele was associated with lower ethylene production and higher air-side lateral root densities (Fig. 4K). This may suggest that TAS Chr8_175425640 is linked to genetic variation that affects *ZmFLA4* function leading to the observed differences in ethylene production.

Complete disruption of ethylene synthesis in two *AtACO* quintuple mutants (*ET-free-1* and *ET-free-2*), in which all five *AtACO* genes were mutated by CRISPR/Cas9 (37), showed a significant increase in air-side lateral root density (Fig. 4L). Similarly, ethylene perception mutants *ein2-5* and *ein2-50* showed a significant increase in air-side lateral root density (Fig. 4M). Together these observations confirm that ethylene suppresses air-side lateral root development. Concomitantly, we observed a decrease in contact-side lateral root density for *ET-free-1*, *ET-free-2*, *ein2-5*, and *ein2-50* that mirrored the increase in air-side lateral root density leading to no change in total lateral root density (fig. S9, I and J). Since lateral root induction can only occur at one of the two xylem poles in Arabidopsis (38), it is possible that a derepression of air-side lateral root development in these mutants leads to lateral root redistribution from the contact-side. While mutants for *EIN2* have not been described in maize, a mutant allele of *OsEIN2* in rice was available and showed a similar defect in hydropatterning as the Arabidopsis mutant alleles (Fig. 4N), providing further evidence that ethylene-dependent regulation of hydropatterning is conserved between Arabidopsis and grasses. A double mutant of ETHYLENE-INSENSITIVE3 (EIN3) and ETHYLENE-INSENSITIVE3-LIKE 1 (EIL1), *ein3/eil1*, two major transcriptional regulators of ethylene signaling that act downstream of EIN2, showed no difference in air-side lateral root density compared to Col-0 wild-type (fig. S9K). This might be due to redundancy in transcriptional regulation or an alternative pathway (39) that leads to air-side suppression of lateral root development by ethylene. Exogenous treatment of *ET-free-1* and *ein2-50* with 0.2 ppm ethylene was sufficient to suppress air-side lateral root development in *ET-free-1*, while *ein2-50* showed no response (Fig. 4, O and P). Our results suggest that localized ethylene synthesis is not necessary and that additional mechanisms must exist that control air-side specific suppression of lateral roots by ethylene.

Since auxin is necessary for lateral root induction and ethylene has been shown to induce local auxin biosynthesis (40), we generated a double mutant of *sos5-2* and *axr1-3* to study their epistatic interactions. While the disruption of auxin signaling leads to an increase in air-side lateral roots, the double mutant *sos5-2/axr1-3* showed a significant decrease in air-side lateral root density (fig. S9L). Our results indicate an additive interaction between auxin and ethylene responses. Further work will be necessary to elucidate how air-side lateral root suppression by ethylene is connected to auxin controlled lateral root induction on the contact-side.

Conclusions

Our results reveal that hydropatterning is a crop-relevant response of roots to heterogeneity in soil moisture. Development of modern breeding germplasm in maize led to the weakening

of hydropatterning in temperate regions, likely through relaxation of selection. This divergence in hydropatterning may relate to the different selection pressures experienced by each subpopulation. Through genetic analyses, we detected associations between hydropatterning and the auxin and ethylene signaling pathways. Dissection of these pathways in maize, rice and Arabidopsis demonstrates that auxin signaling promotes a bias in lateral root development towards moisture-contacting surfaces of the root, while ethylene suppresses branching on air-exposed surfaces (Fig. 4Q and fig. S9M). FLA4, acting at the top of a signaling pathway that restricts ethylene biosynthesis, may perceive an as-of-yet unknown environmental cue to tune the degree to which root architecture is responsive to local soil structure and water availability. Further genetic work in maize is needed to validate our finding from Arabidopsis. A deeper understanding of these pathways may allow for the control of moisture-responsive root growth to improve drought resilience in maize.

Supplementary Material

Refer to Web version on PubMed Central for supplementary material.

Acknowledgments

We gratefully acknowledge the many thoughtful discussions with Virginia Walbot regarding experiments in maize. We thank the USDA-ARS U.S. National Plant Germplasm System for providing the maize seeds from the Goodman-Buckler association panel. Thank you to Samuel Leiboff, Oregon State University, and Carolyn Rasmussen, University of California Riverside, for providing the maize DII-VENUS-NLS reporter lines. We also thank Carolyn Schultz, the University of Adelaide, and Georg Seifert, BOKU Vienna, for discussions regarding the function and role of FLA4. Thank you to Erick Bautista for managing the greenhouse and field facilities at Stanford University, and all members of the Dinneny laboratory for their help with revisions of the draft manuscript.

Funding:

Faculty Scholars grant from the Simons Foundation and Howard Hughes Medical Institute 55108515 (JRD)

Advanced Research Projects Agency-Energy (ARPA-E), U.S. Department of Energy DE-AR 1565-1555 (JRD)

Biological and Environmental Research (BER) Program, U.S. Department of Energy DE-SC0023160 (JRD)

Howard Hughes Medical Institute Investigator award (JRD)

National Science Foundation MCB-2427432 (JK)

UKRI Frontiers Research ERC StG, EP/Y036697/1 (BKP)

Advanced Research Projects Agency-Energy (ARPA-E), U.S. Department of Energy DE-AR 0000826 (PSS)

Biotechnology and Biological Sciences Research Council (BBSRC) BB/V003534/1 to (CJS, JB, MB)

Biotechnology and Biological Sciences Research Council (BBSRC) BB/T001437/1, BB/W008874/1 and BB/W015080/1 (MB)

European Research Council grant HYDROSENSING 101118769 (MB)

HORIZON EUROPE Marie Sklodowska-Curie Actions 765000 (MAV)

EVOTREE project RCN 287465 (SB)

Competing interests:

PSS is a co-founder and CEO of Dryland Genetics, Inc and a co-founder and managing partner of Data2Bio, LLC. He is a member of the scientific advisory boards of Kemin Industries and Centro de Tecnologia Canavieira, as well

as a recipient of research funding from Iowa Corn and Bayer Crop Science. All other authors declare that they have no competing interests.

Data and materials availability:

Data and summary statistics are available in the supplementary materials. Software, raw data and code for image processing, to generate data, statistics, and figures are available on Dryad and Zenodo (41, 42).

References

1. Satoh Y, Yoshimura K, Pokhrel Y, Kim H, Shiogama H, Yokohata T, Hanasaki N, Wada Y, Burek P, Byers E, Schmied HM, Gerten D, Ostberg S, Gosling SN, Boulange JES, Oki T, The timing of unprecedented hydrological drought under climate change. Nat. Commun 13, 3287 (2022). [PubMed: 35764606]
2. Lynch JP, Harnessing root architecture to address global challenges. Plant J. 109, 415–431 (2022). [PubMed: 34724260]
3. Drew MC, Comparison of the effects of a localised supply of phosphate, nitrate, ammonium and potassium on the growth of the seminal root system, and the shoot, in barley. New Phytol 75, 479–490 (1975).
4. Voothuluru P, Wu Y, Sharp RE, Not so hidden anymore: Advances and challenges in understanding root growth under water deficits. Plant Cell 36, 1377–1409 (2024). [PubMed: 38382086]
5. Bao Y, Aggarwal P, Robbins NE 2nd, Sturrock CJ, Thompson MC, Tan HQ, Tham C, Duan L, Rodriguez PL, Vernoux T, Mooney SJ, Bennett MJ, Dinneny JR, Plant roots use a patterning mechanism to position lateral root branches toward available water. Proc Natl Acad Sci U S A 111, 9319–9324 (2014). [PubMed: 24927545]
6. Scharwies JD, Dinneny JR, Water transport, perception, and response in plants. J. Plant Res, doi: 10.1007/s10265-019-01089-8 (2019).
7. Dinneny JR, Developmental Responses to Water and Salinity in Root Systems. Annu Rev Cell Dev Biol 35, 239–257 (2019). [PubMed: 31382759]
8. Flint-Garcia SA, Thuillet A-C, Yu J, Pressoir G, Romero SM, Mitchell SE, Doebley J, Kresovich S, Goodman MM, Buckler ES, Maize association population: a high-resolution platform for quantitative trait locus dissection. Plant J. 44, 1054–1064 (2005). [PubMed: 16359397]
9. Robbins NE 2nd, Dinneny JR, Growth is required for perception of water availability to pattern root branches in plants. Proc Natl Acad Sci U S A 115, E822–E831 (2018). [PubMed: 29317538]
10. Jansen L, Roberts I, De Rycke R, Beeckman T, Phloem-associated auxin response maxima determine radial positioning of lateral roots in maize. Philos. Trans. R. Soc. Lond. B Biol. Sci 367, 1525–1533 (2012). [PubMed: 22527395]
11. Mural RV, Sun G, Grzybowski M, Tross MC, Jin H, Smith C, Newton L, Andorf CM, Woodhouse MR, Thompson AM, Sigmon B, Schnable JC, Association mapping across a multitude of traits collected in diverse environments in maize. Gigascience 11 (2022).
12. Zheng Z, Hey S, Jubery T, Liu H, Yang Y, Coffey L, Miao C, Sigmon B, Schnable JC, Hochholdinger F, Ganapathysubramanian B, Schnable PS, Shared Genetic Control of Root System Architecture between Zea mays and Sorghum bicolor. Plant Physiol. 182, 977–991 (2020). [PubMed: 31740504]
13. Lin H-Y, Liu Q, Li X, Yang J, Liu S, Huang Y, Scanlon MJ, Nettleton D, Schnable PS, Substantial contribution of genetic variation in the expression of transcription factors to phenotypic variation revealed by eRD-GWAS. Genome Biol. 18, 192 (2017). [PubMed: 29041960]
14. Zhan A, Schneider H, Lynch JP, Reduced lateral root branching density improves drought tolerance in maize. Plant Physiol. 168, 1603–1615 (2015). [PubMed: 26077764]
15. Wu Y, San Vicente F, Huang K, Dhliwayo T, Costich DE, Semagn K, Sudha N, Olsen M, Prasanna BM, Zhang X, Babu R, Molecular characterization of CIMMYT maize inbred lines with genotyping-by-sequencing SNPs. Theor. Appl. Genet 129, 753–765 (2016). [PubMed: 26849239]

16. Vasal SK, Mclean S, The Lowland Tropical Maize Subprogram (CIMMYT, 1994).
17. Santure AW, Wang J, The joint effects of selection and dominance on the QST - FST contrast. Genetics 181, 259–276 (2009). [PubMed: 18984567]
18. Orosa-Puente B, Leftley N, von Wangenheim D, Banda J, Srivastava AK, Hill K, Truskina J, Bhosale R, Morris E, Srivastava M, Kümpers B, Goh T, Fukaki H, Vermeer JEM, Vernoux T, Dinneny JR, French AP, Bishopp A, Sadanandom A, Bennett MJ, Root branching toward water involves posttranslational modification of transcription factor ARF7. Science 362, 1407–1410 (2018). [PubMed: 30573626]
19. Kremling KAG, Chen S-Y, Su M-H, Lepak NK, Romay MC, Swarts KL, Lu F, Lorant A, Bradbury PJ, Buckler ES, Dysregulation of expression correlates with rare-allele burden and fitness loss in maize. Nature 555, 520–523 (2018). [PubMed: 29539638]
20. del Pozo JC, Dharmasiri S, Hellmann H, Walker L, Gray WM, Estelle M, AXR1-ECR1-dependent conjugation of RUB1 to the Arabidopsis Cullin AtCUL1 is required for auxin response. Plant Cell 14, 421–433 (2002). [PubMed: 11884684]
21. Liu X, Huang M, Fan B, Buckler ES, Zhang Z, Iterative usage of fixed and random effect models for powerful and efficient genome-wide association studies. PLoS Genet. 12, e1005767 (2016). [PubMed: 26828793]
22. Kusmec A, Schnable PS, FarmCPUpp: Efficient large-scale genomewide association studies. Plant Direct 2, e00053 (2018). [PubMed: 31245719]
23. Lynch M, Ackerman MS, Gout J-F, Long H, Sung W, Thomas WK, Foster PL, Genetic drift, selection and the evolution of the mutation rate. Nat. Rev. Genet 17, 704–714 (2016). [PubMed: 27739533]
24. Su W, Liu Y, Xia Y, Hong Z, Li J, Conserved endoplasmic reticulum-associated degradation system to eliminate mutated receptor-like kinases in *Arabidopsis*. Proc. Natl. Acad. Sci. U. S. A 108, 870–875 (2011). [PubMed: 21187394]
25. Hüttner S, Strasser R, Endoplasmic reticulum-associated degradation of glycoproteins in plants. Front. Plant Sci 3, 67 (2012). [PubMed: 22645596]
26. Shi H, Kim Y, Guo Y, Stevenson B, Zhu J-K, The Arabidopsis SOS5 locus encodes a putative cell surface adhesion protein and is required for normal cell expansion. Plant Cell 15, 19–32 (2003). [PubMed: 12509519]
27. Seifert GJ, The FLA4-FEI pathway: A unique and mysterious signaling module related to cell wall structure and stress signaling. Genes (Basel) 12 (2021).
28. Johnson KL, Jones BJ, Bacic A, Schultz CJ, The fasciclin-like arabinogalactan proteins of Arabidopsis. A multigene family of putative cell adhesion molecules. Plant Physiol. 133, 1911–1925 (2003). [PubMed: 14645732]
29. Xue H, Veit C, Abas L, Tryfona T, Maresch D, Ricardi MM, Estevez JM, Strasser R, Seifert GJ, Arabidopsis thaliana FLA4 functions as a glycan-stabilized soluble factor via its carboxy-proximal Fasciclin 1 domain. Plant J. 91, 613–630 (2017). [PubMed: 28482115]
30. Sigrist CJA, Cerutti L, Hulo N, Gattiker A, Falquet L, Pagni M, Bairoch A, Bucher P, PROSITE: a documented database using patterns and profiles as motif descriptors. Brief. Bioinform 3, 265–274 (2002). [PubMed: 12230035]
31. Chen H, Bullock DA Jr, Alonso JM, Stepanova AN, To fight or to grow: The balancing role of ethylene in plant abiotic stress responses. Plants 11, 33 (2022).
32. Pandey BK, Huang G, Bhosale R, Hartman S, Sturrock CJ, Jose L, Martin OC, Karady M, Laurentius AC, Ljung K, Lynch JP, Brown KM, Whalley WR, Mooney SJ, Zhang D, Bennett MJ, Plant roots sense soil compaction through restricted ethylene diffusion. Science 371, 276–280 (2021). [PubMed: 33446554]
33. Xu S-L, Rahman A, Baskin TI, Kieber JJ, Two leucine-rich repeat receptor kinases mediate signaling, linking cell wall biosynthesis and ACC synthase in Arabidopsis. Plant Cell 20, 3065–3079 (2008). [PubMed: 19017745]
34. Yoshida H, Nagata M, Saito K, Wang KLC, Ecker JR, Arabidopsis ETO1 specifically interacts with and negatively regulates type 2 1-aminocyclopropane-1-carboxylate synthases. BMC Plant Biol. 5, 14 (2005). [PubMed: 16091151]

35. Tsuchisaka A, Yu G, Jin H, Alonso JM, Ecker JR, Zhang X, Gao S, Theologis A, A combinatorial interplay among the 1-aminocyclopropane-1-carboxylate isoforms regulates ethylene biosynthesis in Arabidopsis thaliana. Genetics 183, 979–1003 (2009). [PubMed: 19752216]
36. Polko JK, Kieber JJ, 1-Aminocyclopropane 1-Carboxylic Acid and Its Emerging Role as an Ethylene-Independent Growth Regulator. Front. Plant Sci 10, 1602 (2019). [PubMed: 31921251]
37. Li W, Li Q, Lyu M, Wang Z, Song Z, Zhong S, Gu H, Dong J, Dresselhaus T, Zhong S, Qu L-J, Lack of ethylene does not affect reproductive success and synergid cell death in Arabidopsis. Mol. Plant 15, 354–362 (2022). [PubMed: 34740849]
38. Parizot B, Laplaze L, Ricaud L, Boucheron-Dubuisson E, Bayle V, Bonke M, De Smet I, Poethig SR, Helariutta Y, Haseloff J, Chriqui D, Beeckman T, Nussaume L, Diarch symmetry of the vascular bundle in Arabidopsis root encompasses the pericycle and is reflected in distich lateral root initiation. Plant Physiol. 146, 140–148 (2008). [PubMed: 17993548]
39. Binder BM, Mortimore LA, Stepanova AN, Ecker JR, Bleecker AB, Short-term growth responses to ethylene in Arabidopsis seedlings are EIN3/EIL1 independent. Plant Physiol. 136, 2921–2927 (2004). [PubMed: 15466219]
40. Stepanova AN, Robertson-Hoyt J, Yun J, Benavente LM, Xie D-Y, Dolezal K, Schlereth A, Jürgens G, Alonso JM, TAA1-mediated auxin biosynthesis is essential for hormone crosstalk and plant development. Cell 133, 177–191 (2008). [PubMed: 18394997]
41. Scharwies JD, Clarke T, Zheng Z, Dinneny A, Birkeland S, Veltman MA, Sturrock CJ, Banda J, Torres-Martínez HH, Viana WG, Khare R, Kieber J, Pandey BK, Bennett M, Schnable PS, Dinneny JR, Moisture-responsive root-branching pathways identified in diverse maize breeding germplasm, Zenodo (2024); 10.5281/zenodo.13347148.
42. Scharwies JD, Clarke T, Zheng Z, Dinneny A, Birkeland S, Veltman MA, Sturrock CJ, Banda J, Torres-Martínez HH, Viana WG, Khare R, Kieber J, Pandey BK, Bennett M, Schnable PS, Dinneny JR, Moisture-responsive root-branching pathways identified in diverse maize breeding germplasm, Dryad (2024); 10.5061/dryad.3ffbg79sv.
43. T-DNA Primer Design, Salk Institute Genomic Analysis Laboratory. http://signal.salk.edu/tdnaprimers.2.html.
44. Gioia T, Galinski A, Lenz H, Müller C, Lentz J, Heinz K, Briese C, Putz A, Fiorani F, Watt M, Schurr U, Nagel KA, GrowScreen-PaGe, a non-invasive, high-throughput phenotyping system based on germination paper to quantify crop phenotypic diversity and plasticity of root traits under varying nutrient supply. Funct. Plant Biol 44, 76–93 (2017).
45. Robbins NE, Dinneny JR, A method to analyze local and systemic effects of environmental stimuli on root development in plants. Bio-protocol 6 (2016).
46. Schindelin J, Arganda-Carreras I, Frise E, Kaynig V, Longair M, Pietzsch T, Preibisch S, Rueden C, Saalfeld S, Schmid B, Tinevez J-Y, White DJ, Hartenstein V, Eliceiri K, Tomancak P, Cardona A, Fiji: an open-source platform for biological-image analysis. Nat. Methods 9, 676–682 (2012). [PubMed: 22743772]
47. R Core Team, R: A Language and Environment for Statistical Computing (R Foundation for Statistical Computing, Vienna, Austria, 2022; http://www.R-project.org/).
48. Wickham H, Averick M, Bryan J, Chang W, McGowan L, François R, Grolemund G, Hayes A, Henry L, Hester J, Kuhn M, Pedersen T, Miller E, Bache S, Müller K, Ooms J, Robinson D, Seidel D, Spinu V, Takahashi K, Vaughan D, Wilke C, Woo K, Yutani H, Welcome to the tidyverse. J. Open Source Softw 4, 1686 (2019).
49. Bates D, Mächler M, Bolker B, Walker S, Fitting Linear Mixed-Effects Models Using lme4. J. Stat. Softw 67, 1–48 (2015).
50. Ursache R, Andersen TG, Marhavý P, Geldner N, A protocol for combining fluorescent proteins with histological stains for diverse cell wall components. Plant J. 93, 399–412 (2018). [PubMed: 29171896]
51. Hayashi K, Hasegawa J, Matsunaga S, The boundary of the meristematic and elongation zones in roots: endoreduplication precedes rapid cell expansion. Sci. Rep 3, 2723 (2013). [PubMed: 24121463]
52. Kim S, ppcor: An R Package for a Fast Calculation to Semi-partial Correlation Coefficients. Commun Stat Appl Methods 22, 665–674 (2015). [PubMed: 26688802]

53. Bukowski R, Guo X, Lu Y, Zou C, He B, Rong Z, Wang B, Xu D, Yang B, Xie C, Fan L, Gao S, Xu X, Zhang G, Li Y, Jiao Y, Doebley JF, Ross-Ibarra J, Lorant A, Buffalo V, Romay MC, Buckler ES, Ware D, Lai J, Sun Q, Xu Y, Construction of the third-generation Zea mays haplotype map. Gigascience 7, 1–12 (2018).
54. Danecek P, Auton A, Abecasis G, Albers CA, Banks E, DePristo MA, Handsaker RE, Lunter G, Marth GT, Sherry ST, McVean G, Durbin R, 1000 Genomes Project Analysis Group, The variant call format and VCFtools. Bioinformatics 27, 2156–2158 (2011). [PubMed: 21653522]
55. Danecek P, Bonfield JK, Liddle J, Marshall J, Ohan V, Pollard MO, Whitwham A, Keane T, McCarthy SA, Davies RM, Li H, Twelve years of SAMtools and BCFtools. Gigascience 10 (2021).
56. Quinlan AR, Hall IM, BEDTools: a flexible suite of utilities for comparing genomic features. Bioinformatics 26, 841–842 (2010). [PubMed: 20110278]
57. Li Z, Löytynoja A, Fraimout A, Merilä J, Effects of marker type and filtering criteria on Q ST-F ST comparisons. R Soc Open Sci 6, 190666 (2019). [PubMed: 31827824]
58. Vinayan MT, Seetharam K, Babu R, Zaidi PH, Blummel M, Nair SK, Genome wide association study and genomic prediction for stover quality traits in tropical maize (Zea mays L.). Sci. Rep 11, 686 (2021). [PubMed: 33436870]
59. Purcell S, Neale B, Todd-Brown K, Thomas L, Ferreira MAR, Bender D, Maller J, Sklar P, de Bakker PIW, Daly MJ, Sham PC, PLINK: a tool set for whole-genome association and population-based linkage analyses. Am. J. Hum. Genet 81, 559–575 (2007). [PubMed: 17701901]
60. Alexander DH, Novembre J, Lange K, Fast model-based estimation of ancestry in unrelated individuals. Genome Res. 19, 1655–1664 (2009). [PubMed: 19648217]
61. Liu K, Goodman M, Muse S, Smith JS, Buckler E, Doebley J, Genetic structure and diversity among maize inbred lines as inferred from DNA microsatellites. Genetics 165, 2117–2128 (2003). [PubMed: 14704191]
62. Weir BS, Cockerham CC, Estimating f-statistics for the analysis of population structure. Evolution 38, 1358–1370 (1984). [PubMed: 28563791]
63. Whitlock MC, Lotterhos KE, Reliable Detection of Loci Responsible for Local Adaptation: Inference of a Null Model through Trimming the Distribution of F(ST). Am. Nat 186, S24–36 (2015). [PubMed: 26656214]
64. Da Silva SB, Da Silva A, Pstat: An R package to assess population differentiation in phenotypic traits. R J. 10, 447–454 (2018).
65. Benjamini Y, Hochberg Y, Controlling the false discovery rate: A practical and powerful approach to multiple testing. J. R. Stat. Soc. Series B Stat. Methodol 57, 289–300 (1995).
66. Leiboff S, Li X, Hu H-C, Todt N, Yang J, Li X, Yu X, Muehlbauer GJ, Timmermans MCP, Yu J, Schnable PS, Scanlon MJ, Genetic control of morphometric diversity in the maize shoot apical meristem. Nat. Commun 6, 8974 (2015). [PubMed: 26584889]
67. Bradbury PJ, Zhang Z, Kroon DE, Casstevens TM, Ramdoss Y, Buckler ES, TASSEL: software for association mapping of complex traits in diverse samples. Bioinformatics 23, 2633–2635 (2007). [PubMed: 17586829]
68. Woodhouse MR, Cannon EK, Portwood JL 2nd, Harper LC, Gardiner JM, Schaeffer ML, Andorf CM, A pan-genomic approach to genome databases using maize as a model system. BMC Plant Biol. 21, 385 (2021). [PubMed: 34416864]
69. Phytozome 13, Joint Genome Institute. https://phytozome-next.jgi.doe.gov/.
70. TAIR BLAST 2.9.0+, The Arabidopsis Information Resource (TAIR). https://v2.arabidopsis.org/Blast/.
71. Huang T, Guillotin B, Rahni R, Birnbaum KD, Wagner D, A rapid and sensitive, multiplex, whole mount RNA fluorescence in situ hybridization and immunohistochemistry protocol. Plant Methods 19, 131 (2023). [PubMed: 37993896]
72. Mir R, Aranda LZ, Biaocchi T, Luo A, Sylvester AW, Rasmussen CG, A DII Domain-Based Auxin Reporter Uncovers Low Auxin Signaling during Telophase and Early G1. Plant Physiol. 173, 863–871 (2017). [PubMed: 27881728]

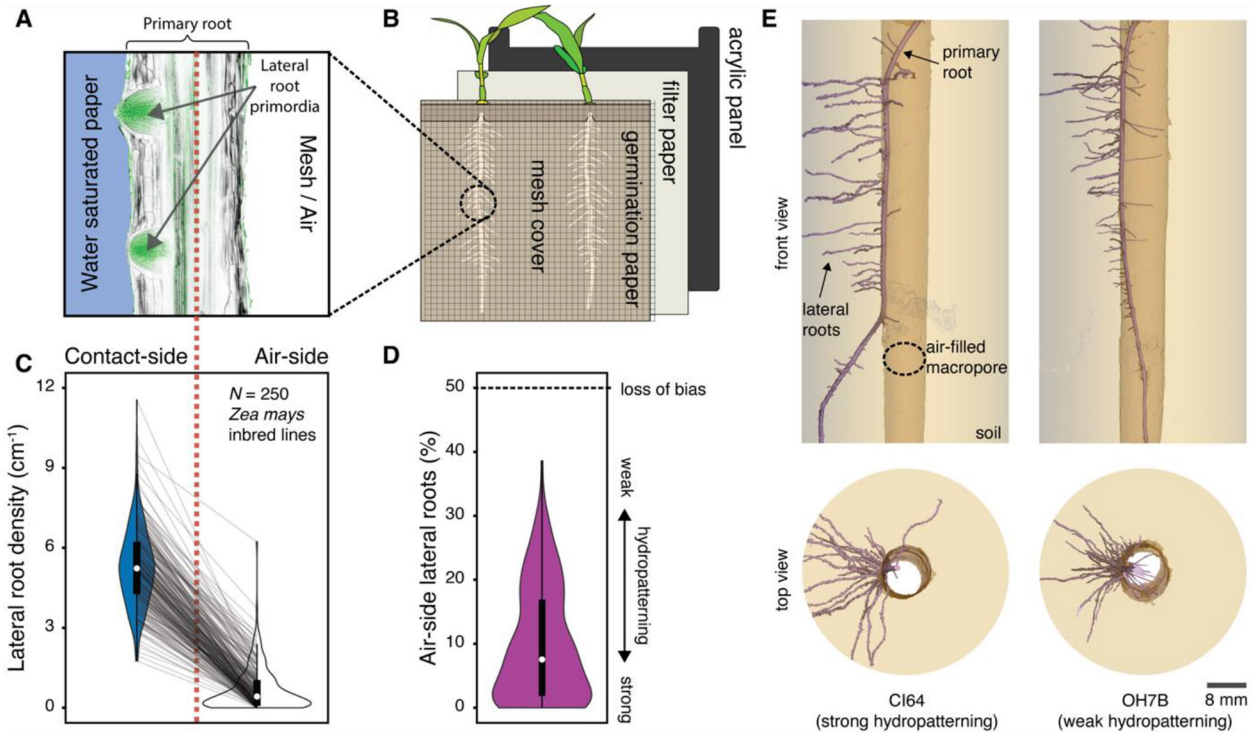

Fig. 1. Hydropatterning responses revealed in public sector breeding lines of *Zea mays* (maize).

(**A and B**) Schematic of the (A) hydropatterning response in (B) our custom-built hydropatterning assay. Primary roots of maize seedlings are grown in a vertical position along moist paper while being prevented from growing off the paper by a mesh cover. Lateral root primordia are preferentially induced towards the water-saturated paper (contact-side) and suppressed on the air-exposed side (air-side). Longitudinal cross-section of maize root (B73 inbred) stained with Calcofluor White (cell walls; gray) and SYBR Green (lateral root primordia; green). Contact- and air-side are separated by a dashed red line. (**C and D**) Distribution of (C) contact- (blue) and air-side (white) lateral root densities from 250 maize inbred lines characterized using the hydropatterning assay and calculated (D) percent air-side lateral roots (purple). Each inbred line is represented by its median value (n = 1 – 3 seedlings/inbred) (data S2). Gray lines connect corresponding inbred lines. Population median (white circles). (**E**) 3D rendered X-ray Computed Tomography images, viewed from the front and the top, showing lateral root patterning on primary roots of strong (CI64) and weak (OH7B) hydropatterning inbred lines grown through an air-filled macropore in soil.

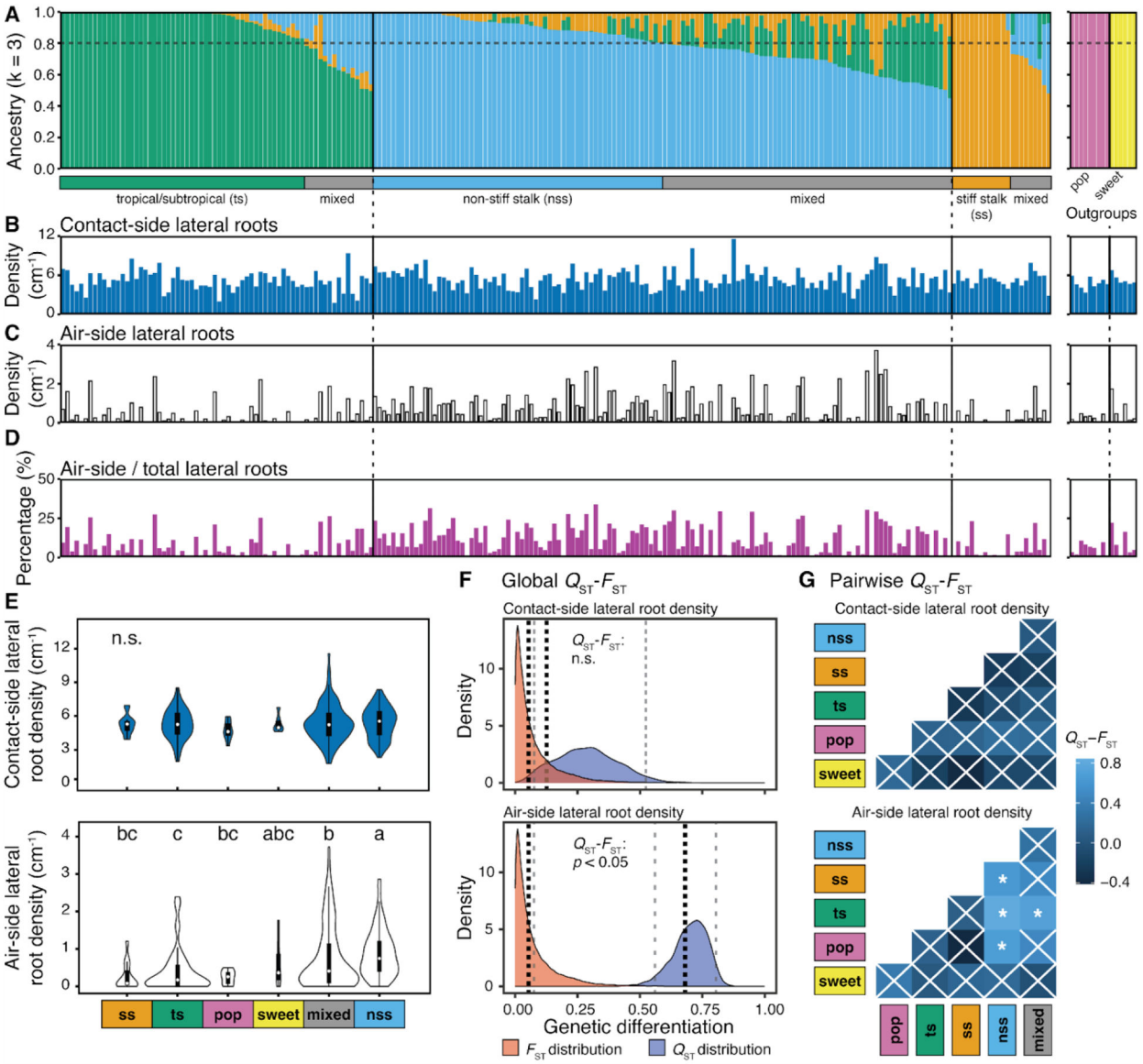

Fig. 2. Differences in hydropatterning across breeding subpopulations may have been caused by divergent selection.

(**A - D**) Population structure and hydropatterning traits of 231 maize inbred lines (19 inbred lines from original population of $N = 250$ were excluded due to missing genotypic data). (A) Ancestry components and subpopulation assignments. Inbred lines < 80% group identity = “mixed”. Popcorn (pop) and sweet corn (sweet) groups were defined a priori. Phenotypic data of (B) contact-side and (C) air-side lateral root density, and (D) percent air-side lateral roots are shown as the median value for each inbred line ($n = 1 – 3$ seedlings/inbred) (data S2). (**E**) Subpopulation comparisons of contact-side (top) and air-side (bottom) lateral root density. Violin plot area adjusted for number of inbred lines/subpopulation. Letters denote significant differences between subpopulations ($p \leq 0.05$, Kruskal–Wallis and Dunn’s post hoc tests); n.s., no significant differences. (**F**) Population-wide comparison of F_{ST} (fixation index) and Q_{ST} (genetic differentiation regarding a quantitative trait) distributions

for contact-side (top) and air-side (bottom) lateral root density. Black dotted lines (means), gray dashed lines (95% confidence intervals). (**G**) Subpopulation pairwise Q_{ST} - F_{ST} comparisons. Asterisks denote significant differences between Q_{ST} and F_{ST} (Benjamini & Hochberg-adjusted: * $p \leq 0.05$); white crosses, not significant. Number of inbred lines in each subpopulation across all panels: $n_{ts} = 53$, $n_{nss} = 63$, $n_{ss} = 14$, $n_{mixed} = 88$, $n_{pop} = 9$, $n_{sweet} = 6$.

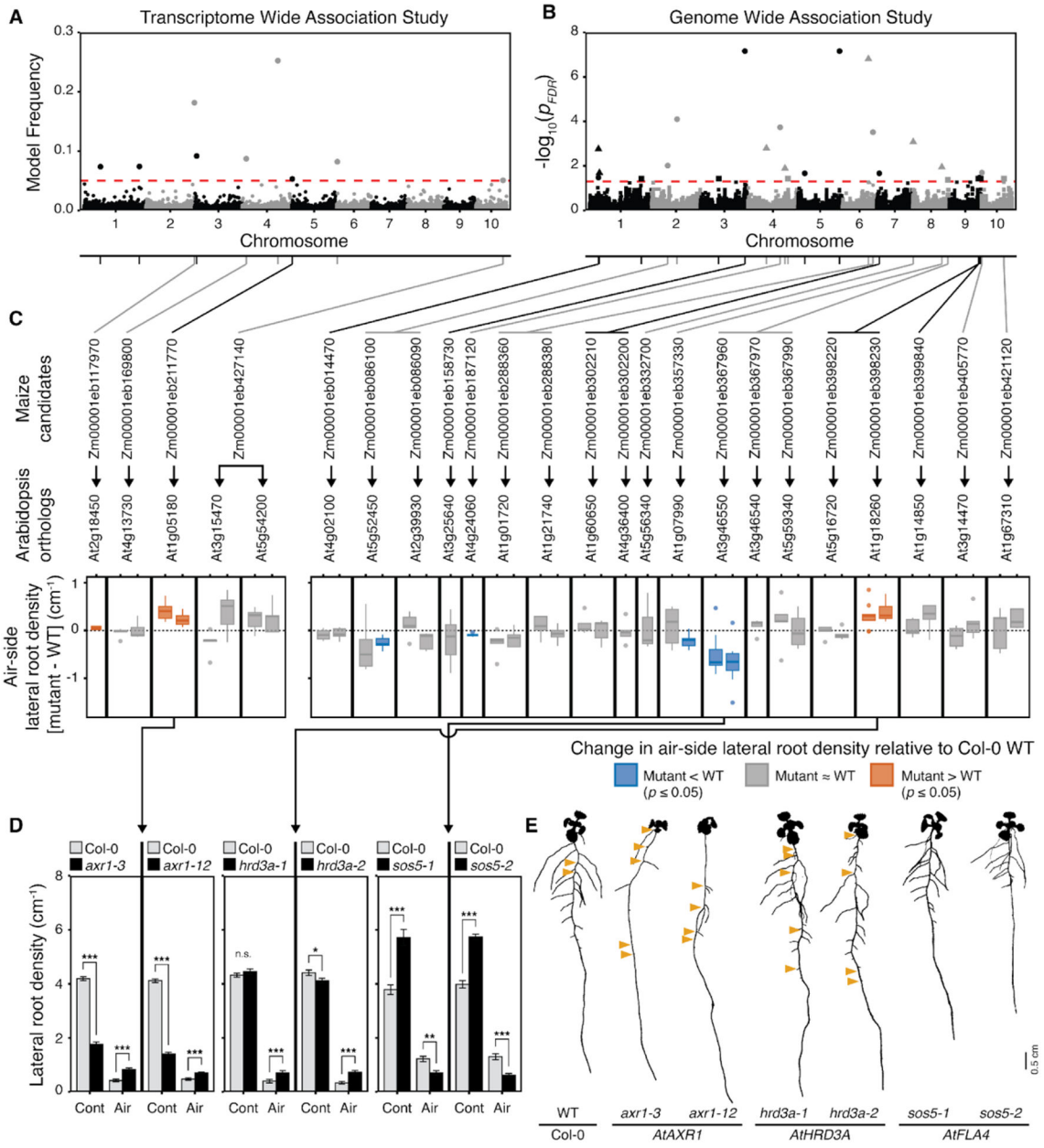

Fig. 3. Genetic control for hydropatterning revealed in maize and validated in Arabidopsis.

(**A and B**) Manhattan plots of Transcriptome Wide Association Study (TWAS) and Genome Wide Association Studies (GWAS) for air-side lateral root density in maize. (A) TWAS used gene expression data from maize root tips (19). Significance threshold: model frequency = 0.05 (red dashed line). (B) GWAS shows smallest *p*-value for each Single Nucleotide Polymorphism (SNP) across three Minor Allele Frequency cutoffs ≥ 0.4% (solid circles), ≥ 2.2% (solid triangles), and ≥ 4.4% (solid squares). FDR-adjusted significance threshold: $p = 0.05$ (red dashed line). Gray/black lines connect SNPs and associated candidate genes corresponding to the chromosome coloration. (**C**) Validation of maize candidate genes using mutants of corresponding gene orthologs in Arabidopsis. Air-side lateral root densities of mutants are shown relative to Col-0 wild-type (WT). Fill color denotes significant

differences (Paired Student's t-test, $p \leq 0.05$) mutants > WT (orange), mutants < WT (blue), not significant (gray) $n = 5 – 10$ plates per mutant (5 WT & 5 mutant seedlings/plate). (**D**) Comparisons of contact-side (Cont) and air-side (Air) lateral root densities between Col-0 wild-type (gray) and mutants for *AtAXR1*, *AtHRD3A*, and *AtFLA4* (all mutants black). $n = 10$ plates per mutant (5 WT & 5 mutant seedlings/plate). Asterisks denote significant differences (Paired Student's t-test: * $p \leq 0.05$, ** $p \leq 0.01$, *** $p \leq 0.001$). Bar graphs: mean +/− SEM. (**E**) Binary images of 11 days-old seedlings. Orange triangles mark air-side lateral roots. Scale bar = 0.5 cm. Dilation was used on images to improve visibility.

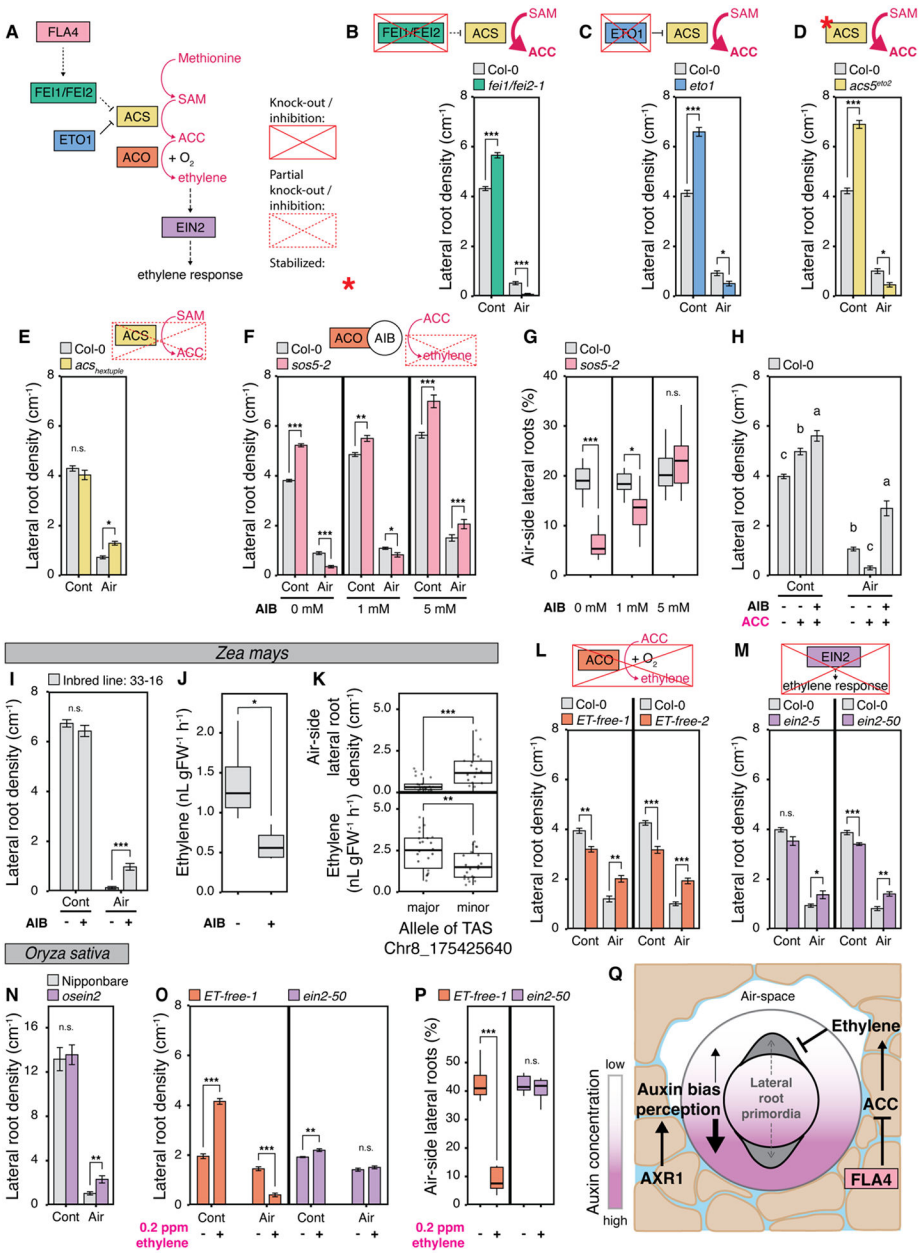

Fig. 4. Ethylene inhibits formation of air-side lateral roots in Arabidopsis, maize, and rice.

(**A**) FLA4 and the ethylene pathway in Arabidopsis (27). (**B - E**) Contact- (Cont) and air-side (Air) lateral root densities in Arabidopsis mutants (C) *eto1* (blue, n = 5 plates), (D) *acs5*^{eto2} (yellow, n = 5 plates), and (E) *acs2-1/4-1/5-2/6-1/7-1/9-1* hextuple mutant (yellow, n = 5 plates) relative to Col-0 (gray). (**F and G**) Effect of 2-Aminoisobutyric acid (AIB) on Arabidopsis mutant *sos5-2* relative to Col-0 (pink, n = 10 plates/treatment). (**H**) Arabidopsis Col-0 response to ACC, AIB, and combination: (–) mock control and (+) 0.05 mM ACC / 5 mM AIB; n = 10 plates/treatment. Letters denote significant differences between treatments (ANOVA, post-hoc Tukey HSD Test). (**I and J**) Response of maize inbred 33–16 to (+) 10 mM AIB relative to (–) mock control (n = 20 plants/treatment), and related ethylene production (n = 4 samples of five roots/treatment). (**K**) Air-side lateral root density and

root ethylene production for maize inbred lines (n = 22/allele) with the major (G) or minor (T) allele at TAS Chr8_175425640. (**L - N**) Contact- and air-side lateral root densities in Arabidopsis mutants (L) *ET-free-1* & *ET-free-2* (orange, n = 8 – 9 plates) and (M) *ein2-5* & *ein2-50* (purple, n = 10 plates) relative to Col-0, and in (N) rice mutant *osein2* (purple, n = 11 seedlings) relative to Nipponbare wild-type (gray, n = 16 seedlings). (**O and P**) Effect of exogenous ethylene treatment on Arabidopsis mutants *ET-free-1* (n = 8 plates/treatment) and *ein2-50* (n = 8 plates/treatment). (**Q**) Working model of hydropatterning controlled by auxin and ethylene. Asterisks denote significant differences (Student's t-test: * $p \leq 0.05$, ** $p \leq 0.01$, *** $p \leq 0.001$), n.s., not significant. Bar graphs: mean +/− SEM.